JNeurosci
THE JOURNAL OF NEUROSCIENCE

Research Articles: Systems/Circuits

Non-synaptic transmission mediates light context-dependent odor responses in *Drosophila melanogaster*

https://doi.org/10.1523/JNEUROSCI.1106-22.2022

Cite as: J. Neurosci 2022; 10.1523/JNEUROSCI.1106-22.2022

Received: 6 June 2022
Revised: 23 September 2022
Accepted: 26 September 2022

Non-synaptic transmission mediates light context-dependent odor responses in *Drosophila melanogaster*

Abbreviated title: Ephaptic transmission over long distance

Kazuaki Ikeda[1,2,#], Masaki Kataoka[1,2,#], Nobuaki K. Tanaka[1,2,3,*]

[1]Division of Biology, Department of Biological Sciences, School of Science, Hokkaido University, North 10, West 8, Kita-ku, Sapporo 060-0810, Japan

[2]Graduate School of Life Sciences, Hokkaido University, North 10, West 8, Kita-ku, Sapporo 060-0810, Japan

[3]Faculty of Science, Hokkaido University, North 10, West 8, Kita-ku, Sapporo 060-0810, Japan

[#]These authors equally contributed.

[*]Correspondence: nktanaka@sci.hokudai.ac.jp (N.K.T.)

Number of Pages: 19

Number of figures: 4

Number of tables: 1

Number of multimedia: 0

Number of extended data: 0

Number of words: Abstract (124), Introduction (542), and Discussion (618)

Conflict of interest:

The authors declare no competing financial interests.

Author contributions:

KI, MK, and NKT designed research, acquired, and analyzed data, and wrote the paper.

Acknowledgments:

This work was supported by PRESTO, Japan Science and Technology Agency and by Grant in-Aid for Scientific Research from the Ministry of Education, Culture, Sports, Science, and Technology of Japan to N.K.T. (grant numbers: 22770068, 24120509, 26830026, 17K07480, and 20K06733). We would like to thank Fumika Hamada, Akiko Sato, Takahiro Chihara, Kazuhiko Kume, Taro Ueno, Ryusuke Niwa, Tadao Usui, Leslie Vosshall, Barry Dickson, Sarah Certel, the Kyoto *Drosophila* Genetic Resource Center, and the Bloomington *Drosophila* Stock Center for providing fly strains. We appreciate Ayumi Tanaka and Ryoichi Tanaka in measuring light intensities; Shuzo Sakata in critically reading the manuscript; and Makoto Mizunami, Joby Joseph, and members of the Hokto Kazama laboratory for helpful suggestions.

Abstract

Recent connectome analyses of the entire synaptic circuit in the nervous system have provided tremendous insights into how neural processing occurs through the synaptic relay of neural information. Conversely, the extent to which ephaptic transmission which does not depend on the synapses contributes to the relay of neural information, especially beyond a distance between adjacent neurons and to neural processing remains unclear. We show that ephaptic transmission mediated by extracellular potential changes in female *Drosophila melanogaster* can reach more than 200 μm, equivalent to the depth of its brain. Furthermore, ephaptic transmission driven by retinal photoreceptor cells mediates light-evoked firing rate increases in olfactory sensory neurons. These results indicate that ephaptic transmission contributes to sensory responses that can change momentarily in a context-dependent manner.

Significance Statement

Although extracellular field potential activities are commonly observed in many nervous systems, this activity has been generally considered as a side effect of synchronized spiking of neurons. This study, however, shows that field potential changes in retinae evoked by a sensory stimulus can control the excitability of distant neurons in vivo and mediates multimodal sensory integration in *Drosophila melanogaster*. As such ephaptic transmission is more effective at a short distance, the ephaptic transmission from the retinae may contribute significantly to firing rate changes in downstream neurons of the photoreceptor cells in the optic lobe.

Introduction

Behavioral responses to a specific mode of sensory input varies with the context. For example, in *Drosophila melanogaster*, pairing a food odor with a visual stimulus enhanced the optomotor response (Chow et al., 2011), and light facilitated both establishment and recall of olfactory memory (Yarali et al., 2008). Sensory information from different modalities is generally integrated by sensory neurons expressing multimodal sensory receptors or by the convergence of synaptic relay of sensory information originating from distinct sensory organs onto individual neurons (van Atteveldt et al., 2014). This study demonstrates that ephaptic transmission also contributes to sensory integration.

Ephaptic transmission is a form of communication that does not depend on synapses. It is mediated by changes in extracellular field potential or electric field, evoked by neural activity (Weiss and Faber, 2010; Buzsáki et al., 2012; Anastassiou and Koch, 2015). Recent studies have reported that excitation of an olfactory sensory neuron (OSN) induces ephaptic inhibition in another OSN housed in the same sensillum in *Drosophila* antennae (Zhang et al., 2019), and that firing of a Purkinje cell promotes synchronous firing of nearby Purkinje cells by ephaptic coupling (Han et al., 2018). These findings reveal the existence of ephaptic transmission between neighboring neurons. However, the contribution of ephaptic transmission at a distance remains unclear in vivo, as it is not easy to separate the effect of ephaptic communication from synaptic communication. To study this further, we analyzed the integration of visual and olfactory inputs in *Drosophila*.

In *Drosophila*, light is primarily received by external photoreceptor cells in the compound eyes and ocelli. Moreover, internal photoreceptor cells in Hofbauer-Buchner eyelets and brain also contribute to sensing light to regulate the circadian rhythm (Malpel et al., 2002; Yasuyama and Meinertzhagen, 1999; Ni et al., 2017). In contrast, olfactory sensory input is received by OSNs in the antennae and maxillary palpi. OSNs send projections to the primary olfactory center, referred to as the antennal lobe (Wilson, 2013). Dye injection into the antennal lobe does not label the optic lobe (i.e., the primary visual center), indicating that there are no direct connections between the primary olfactory and visual centers (Tanaka et al., 2012). The

mushroom body is considered as the site of integration of visual and olfactory information, since it is connected to the primary centers and its intrinsic neurons respond to light and odor stimulations (Yagi et al., 2016; Vogt et al., 2016). However, it remains unclear if peripheral sensory neurons integrate visual and olfactory information.

In this study, we recorded odor and light responses from OSNs expressing the olfactory receptor Or67d, under various light conditions (Fig. 1A). Or67d OSN is the sole OSN housed in the trichodia sensillum1 (T1), the largest spine-shaped sensillum distributed in the proximal part of the antenna (Shanbhag et al., 1999). Or67d OSN responds specifically to the male pheromone *cis*-vaccenyl acetate (cVA), and the spikes recorded from T1 sensilla are composed of a single unit of the Or67d OSN (van Naters and Carlson, 2007), which enabled us to record the same type of neuron repeatedly from different individuals. Analyses of the firing patterns of Or67d OSNs revealed that a transient change in the light condition modified the odor response of Or67d OSNs, which was mediated by ephaptic transmission driven by retinal photoreceptor cells.

Materials and Methods

Drosophila strains

Flies were reared on standard agar-cornmeal medium at 25°C with a 12-hour light/12-hour dark cycle. We used female flies between 3 to 7 days after eclosion.

We used Canton S as a wild type and the following mutants for the single-sensillum recordings: eya^{2} (RRID: BDSC_2285; Choi and Benzer, 1994), hdc^{JK910} (RRID: BDSC_64203; Burg et al., 1993; Melzig et al., 1996), and $norpA^{36}$ (RRID: BDSC_9048; Bloomquist et al., 1988) obtained from the Bloomington *Drosophila* Stock Center (BDSC). We prepared flies in which synaptic transmission of the photoreceptors in the ocelli, compound eyes, and eyelets were blocked by mating *longGMR-GAL4* (RRID: BDSC_8121; Wernet et al., 2003) from BDSC with *UAS-tetanus toxin* (TNT; BDSC_28838; Sweeney et al., 1995) gifted by Aki Ejima. To label the photoreceptor cells, flies bearing both *UAS-GFP*

obtained from Barry Dickson (Tanaka et al., 2008) and *UAS-20XmCD8::GFP* from BDSC (RRID: BDSC_32194) were crossed with *longGMR-GAL4*.

Single-sensillum recording from the antennal T1 sensillum

Each female fly was anesthetized in a vial on ice for less than 1 min and restrained in a custom-made plastic dish by fixing the appendages with wax and epoxy (Tanaka et al., 2009). The right antenna was then set on a tin foil to which the rear side of the antenna was bonded with epoxy to avoid movement. To exclude the light, the head except for the right antenna was painted with black acrylic paint. While the epoxy and paint were drying, the dish was placed in a moist chamber for 15–20 min in the dark. The lateral surface of the thorax was then gently heated using a wax melter to avoid muscle movement in the thorax. After applying *Drosophila* saline (in mM: NaCl 103, KCl 3, N-tris(hydroxymethyl)methyl-2-aminoethanesulfonic acid 5, trehalose 10, glucose 10, sucrose 7, $NaHCO_3$ 26, NaH_2PO_4 1, $CaCl_2$ 1.5, $MgCl_2$ 4, adjusted to pH 7.25 with HCl) over the thorax, the cuticle of the thorax was partially removed. Surgical manipulations such as transplantation of a compound eye were performed using a window made on the top of the head in saline. After removing fat and air sacs over the brain through the window, saline was applied over the brain. For the transplantation experiment, a compound eye severed from a wild-type female fly by cutting the rim of the eye was set on the window. The outer surface of the eye was kept dry. To amputate the antennal nerve, we inserted forceps through the window and cut the right antennal nerve. All dissection steps were performed with forceps under a dissection microscope.

The restrained fly was then placed under a Slicescope (Scientifica, East Sussex, UK) equipped with a GSWH20x/12.5 ocular lens, LUCPlanFLN40x (n.a. 0.60) objective and U-ECA 2x magnification changers (Olympus, Tokyo, Japan). When recording spikes from the T1 sensillum, the recording and reference electrodes were inserted into the base of the sensillum and into saline over the thorax, respectively. We inserted the reference electrode into saline, instead of the head, to avoid recording light-evoked potentials through the reference electrode. To inject current, we additionally inserted a

tungsten electrode that were connected to an AxoClamp-2B (Molecular Devices, San Jose, CA, USA) into the right optic lobe area. We recorded neural responses from a single sensillum in each animal. The recording electrodes (impedance of approximately 90 MΩ) were prepared by pulling quartz capillaries (QF100-70-7.5, Sutter Instrument, Novato, CA, USA) with a Sutter Instrument P2000 puller and filled with sensillum lymph ringer (in mM: KCl 171.9, KH_2PO_4 9.2, K_2HPO_4 10.8, MgCl 3, $CaCl_2$ 1, glucose 22.5, NaCl 25, adjusted to pH 6.5 with HCl) (Kaissling and Thorson, 1980; Dobritsa et al., 2003; Olsson and Hansson, 2013).

Recorded signals were amplified 100-fold with a headstage (8024/7001 N=1, Dagan Corporation, Minneapolis, MN, USA) and DAGAN 8700 Cell Explorer amplifier, and were fed into a PC via an A/D converter Digidata 1322A or 1440A (Molecular Devices). Data was filtered digitally between 65 and 5 kHz using the Axoscope software (Molecular Devices). All recorded data were analyzed using MATLAB 2019b (The MathWorks, Inc., Natick, MA, USA). Recordings under each light condition was repeated three to five times for each animal, and the firing rates were averaged for further analyses. In animals transplanted with a compound eye, data was excluded if the average firing rate in a 300-ms bin just before the light stimulations differed by more than 5 Hz between trials, with and without light stimulation.

Odor and light stimulations

For the odor stimulations, an air puff (3 s, 240 mL/min) from a pneumatic picopump (PV 820, World Precision Instruments, Sarasota, FL, USA) that passed through a tube inserted with filter paper (3.5 x 50 mm) containing 15 µL of either paraffin oil or 1% v/v cVA in paraffin oil was applied to a fly every 30 s. The airpuff speed was adjusted to 1 m/s. Odorized air was continuously removed using a vacuum tube set near the fly's body. The total amount of cVA in the oil was adjusted to 140 µg.

Flies were subjected to 1.5 s light-on or light-off stimulations simultaneously with odor stimulations. Emitted light from an Olympus U-HGLGPS mercury lamp was filtered by U-MNIBA3 which allows 470–495 nm light to pass, and the intensity was adjusted to 55 µmol m^{-2} s^{-1}. We confirmed

these values using a LI-250 light meter connected to an LI-190SA quantum sensor (LI-COR, Lincoln, NE, USA). The picopump and shutter were controlled using Master-8 (A.M.P.I., Jerusalem, Israel). We randomly alternated the order of different light conditions and counterbalanced the number of recordings of one light condition preceding the other, with those in the opposite sequence.

Antibody staining of the brain

Brains were dissected in phosphate buffered saline (PBS) and fixed in 4% paraformaldehyde in PBS for 60 min. After washing with PBS, the brains were shaken in a blocking solution: 10% goat serum in 0.2 % triton in PBS (PBST). They were subsequently incubated overnight in the blocking solution containing primary antibodies at room temperature with shaking. After washing with 0.2% PBST, the brains were incubated overnight in the blocking solution containing secondary antibodies at room temperature with shaking. Finally, the brains were washed with PBS and mounted in Vectashield mounting medium (Vector Laboratories, Inc., Burlingame, CA, USA).

The primary antibodies used were rabbit anti-GFP (A-11122, Molecular Probes, Eugene, OR; RRID: AB_221569; diluted at 1:500) and mouse anti-choline acetyltransferase antibodies (Takagawa and Salvaterra, 1996; 4B1, Developmental Studies Hybridoma Bank at University of Iowa, USA; RRID: AB_528122; 1:200). Goat anti-rabbit antibodies conjugated with Alexa Fluor 488 (A11034, Life Technologies Japan LTD, Tokyo, Japan; RRID: AB_2576217; diluted at 1:200) and anti-mouse antibodies with Alexa Fluor 568 (A11004, Life Technologies Japan LTD; RRID: AB_2534072; 1:200) were used as the secondary antibodies.

Reconstruction and analyses of confocal images

Confocal serial optical images were taken at 0.9–3.8 μm z intervals with a Carl Zeiss (Jena, Germany) LSM 700 laser scanning confocal microscope equipped with Plan-Neofluar 20×/0.50 and C-Apochromat 40×/1.2W lenses. Three-dimensional reconstruction of confocal images was performed with Zeiss ZEN

2012. The brightness, color, and contrast of images were adjusted with Photoshop CS 5.1 (Adobe Inc., San Jose, CA, USA).

The confocal microscope was also used to measure the distance between the bottom of the transplanted eye and the top of the brain immediately after recording the odor responses from *eya*^{2} mutants transplanted with a compound eye from a wild-type fly.

Experimental design and statistical analysis

Data are presented as mean ± SEM. We performed Wilcoxon matched-pairs signed rank test and Mann-Whitney test using Prism 5 (GraphPad, San Diego, CA, USA). We calculated *r* correlation coefficients as effect sizes on R 4.2.1 (https://www.R-project.org/) by dividing *Z* statistic by the square root of the total number of animals. We used G*Power 3.1 (Faul et al., 2007) to perform power analysis. We calculated the minimum sample sizes required to detect enough statistical power (0.8) during the period II in Fig. 2A, 3D, 3E, 4A, and 4D that showed firing rate increases during sustained lighting or current injection. The mean minimum sample size was approximately 7. We thus considered that the sample size of 7 was enough to detect a positive result during the period II. Statistical significance was set at $p < 0.05$. *p*-values, *r*-values, and sample sizes are shown in the figures and Table 1.

Results

Effect of transient changes in light condition on the odor response pattern of Or67d OSNs

We first investigated whether light conditions affected the response to cVA in Or67d OSNs and found that 1.5-s blue light stimulations transiently applied in the dark during the latter half of 3-s odor stimulations decreased the firing rate by 12 Hz on an average, at the onset of light. The firing rate then increased by 2–3 Hz until the offset of light (Figs. 1B and 2A). Conversely, when the flies were set under constant blue light and subjected to transient darkening during the latter half of odor stimulation, we observed an increase in the firing rates at light offset and then a gradual decrease until the onset of light (Fig. 2B). When flies were

212 subjected to blue light stimulation alone in the dark without odor stimulation, a significant change in the
213 firing rate was observed only at the offset when the firing rate was increased (Fig. 2C). However, significant
214 firing rate changes were not observed when blue light stimulation was applied transiently in the dark during
215 the first half of cVA stimulation (Fig. 2D). This may be because the firing rate drastically changed during
216 the first half of cVA stimulation, which may have obscured the effect of light stimulation. We also did not
217 observe significant differences in the firing rates during cVA stimulation between constant light and
218 constant dark conditions (Fig. 2E). These results suggest that transient changes in light conditions altered
219 the odor response patterns of Or67d OSNs, especially when the firing rate in the OSNs was nearly constant.
220 As a thermistor placed under the blue light did not show any temperature changes, the firing rate changes
221 were caused by photoreception. The firing rates of Or67d OSNs during odor stimulation decreased at the
222 onset of light and increased at the offset. Moreover, between the onset and offset, the firing rate increased
223 during sustained lighting but decreased during sustained darkening.

224

225 **Antennal photoreceptors contributing to the light-evoked firing rate changes in Or67d OSNs at the**
226 **onset and offset of light**

227 We next examined the neural mechanisms underlying light-evoked firing rate changes in the OSNs. We
228 focused on the firing rate changes observed by blue light stimulations which were transiently applied in the
229 dark during the latter half of odor stimulations in which light-evoked firing rate changes were clearly
230 observed. To determine if antennal photoreceptors contribute to these changes, we recorded from wild-type
231 flies whose antennal nerve which connects the antenna and brain was severed, and flies whose heads were
232 covered with black paint, except for one antenna for recording (Fig. 3A, B). Neither fly exhibited an
233 increase in firing rate during sustained light, indicating that the increase involves photoreceptors outside the
234 antennae. However, we observed light-evoked firing rate changes at the onset and offset of light in these
235 flies, although the change at the onset was not statistically significant in the painted flies (Fig. 3B). These
236 results indicate that while the firing rate changes at light onset and offset occur autonomously within the

antenna, the photoreceptors within the antennae contribute little to the firing rate increase between onset and offset.

Ephaptic transmission from the compound eyes contributes to the light-evoked firing rate increases in Or67d OSNs during sustained light

We next examined the contribution of photoreceptors outside the antennae to the firing rate increases during sustained light. We first analyzed *eyes absent* (*eya*^{2}) mutants that lacked compound eyes, but not ocelli (Choi and Benzer, 1994), and did not observe an increase in firing rates in the *eya*^{2} mutants (Fig. 3C). We further analyzed two strains in which chemical transmission of photoreceptors in the compound eyes was blocked: *histidine decarboxylase* mutants (*hdc*^{JK910}) that lacked histamine, a neurotransmitter of the photoreceptor cells in the compound eyes (Burg et al., 1993; Melzig et al., 1996) (Fig. 3D), and *longGMR-GAL4*/*UAS-tetanus toxin* mutants, in which chemical synaptic transmission of cholinergic photoreceptor cells in Hofbauer-Buchner eyelets was blocked (Yasuyama and Meinertzhagen, 1999) as well as photoreceptor cells in the compound eyes and ocelli (Fig. 3E-I). These two strains exhibited normal light-evoked firing rate changes, except at light onset in *hdc*^{JK910}. This result appears to contradict the findings in the *eya*^{2} mutants, but also raises the possibility that although photoreception by the photoreceptor cells in the compound eyes were indispensable, synaptic transmission from photoreceptor cells was not necessary for the light-evoked firing rate increases during sustained lighting.

We therefore verified whether synaptic relay of information from photoreceptor cells in the compound eyes was required for increasing the light-evoked firing rate. We prepared *eya*^{2} mutants in which a compound eye severed from a wild-type fly was placed on a window made at the top of the head cuticle. Synaptic relay of light information through both chemical and electrical synapses from the transplanted compound eye to the brain were completely missing in *eya*^{2} mutants that were operated on. The operated *eya*^{2} mutants showed the light-evoked firing rate increase comparable to that of the wild type (Fig. 4A). This result indicates that the mechanisms that evoke firing rate changes in the OSNs are normal in the *eya*^{2}

mutants except for photoreception in the compound eyes. The increase in firing rate were not induced by surgical manipulation, as the firing rate did not increase in *eya*^{2} mutants transplanted with the compound eye of a *no receptor potential A* mutant (*norpA*^{36}), in which the phototransduction pathway in photoreceptor cells is disrupted due to dysfunction of *phospholipase C-β* gene (Bloomquist et al., 1988; Pearn et al., 1996) (Fig. 4B). Consistent with observations in *hdc*^{JK910} and *longGMR-GAL4/UAS-tetanus toxin* flies, this result demonstrates that synaptic relay of light information from the compound eyes to brain is not required to increase the firing rate. Furthermore, since we did not manipulate the brain of these operated *eya*^{2} mutants, the photoreceptors within the brain were unlikely to contribute to the increase in firing rate during sustained lighting.

We further investigated whether diffusion of chemical substances released from the transplanted compound eye, induced an increase in firing rate in the OSNs. For this purpose, a tungsten wire connected to the ground was inserted into extracellular saline covering the *eya*^{2} brain, to minimize light-evoked extracellular field potential change near the transplanted compound eye, without interrupting the diffusion of chemical substances from the compound eye or the blue light path to the compound eye and brain. In such preparations, we did not observe an increase in the firing rate during sustained light (Fig. 4C), although we observed normal cVA responses in OSNs. This indicates that the light-evoked firing rate increase was not mediated by chemical substances released from the compound eye. We also examined whether negative filed potential deflections in the optic lobe area were also able to induce an increase in firing rate in the OSNs, as light evokes negative field potential deflections in the retina (Pearn et al., 1996). We found that a negative current (-10 nA) injected into the optic lobe area in *eya*^{2} mutants caused an increase in firing rate (Fig. 4D). Thus, we conclude that ephaptic transmission, but not synaptic transmission from the photoreceptor cells, mediated by field potential changes in the retina, induced light-evoked firing rate increase of OSNs in the antennae. The transplanted eye was separated from the brain and antennae by a distance of more than 200 μm, indicating that field potential change evoked by retinal activity has the potential to change the spiking patterns of distant neurons in the fly brain.

287

288 **Discussion**

289 We found that ephaptic transmission of light information from photoreceptor cells in the retina mediates the
290 increase in firing rate in the OSNs during odor stimulations. This study has not revealed whether the
291 ephaptic transmission directly changes the firing rate of the OSNs. We observed that amputation of the
292 antennal nerve abolished the firing rate increases during sustained light (Fig. 3A), suggesting that once the
293 light information might be received by neurons in the brain, the information would be relayed by the
294 neurons through the antennal nerve to the antenna, resulting in the firing rate increases in the OSNs.

295 While ephaptic coupling has been reported earlier such as between neighboring neurons within
296 the same sensillum, or between Purkinje cells, which is at a distance of less than 100 µm (Su et al., 2013;
297 Han et al., 2018), this study shows that ephaptic transmission reaches over 200 µm in vivo, equivalent to the
298 depth of the entire fly brain, beyond the distance between neighboring neurons. Light stimulations cause
299 ~-10 mV field potential deflections in a retina (Pearn et al., 1996). If we neglect endogenous fields in the
300 brain, light stimulations may induce ~33.3 mV/mm electric field between the retina and center of the brain
301 (0 mV), since the distance between them is 300 µm approximately. This electric field is strong enough to
302 modulate neural activities, as even weaker electric fields (<0.5 mV/mm) changed the firing patterns of
303 neurons in vitro (Weiss and Faber, 2010).

304 In rodents, the firing rate of cerebellar Purkinje cells either decreased or increased when a
305 current was injected into the extracellular field around their axons, causing field potential changes of 0.2
306 mV (Blot and Barbour, 2014). In insects, odor-evoked field potential oscillations whose amplitude is
307 comparable to that caused by the current injection in the rodents, are induced by synchronous firing of
308 olfactory neurons in the antennal lobe which are mediated by GABAergic neurons forming reciprocal
309 synapses with excitatory projection neurons (Stopfer et al., 1997; Tanaka et al., 2009). Changes in the
310 extracellular field potential are commonly observed in many nervous systems (Buzsáki et al., 2012). While

311 such extracellular field potential activities have been considered as a side effect of synchronized spiking of
312 neurons, this study suggests that such field potential changes evoked by a sensory stimulus can control the
313 excitability of distant neurons, in addition to adjacent neurons. As ephaptic transmission is more effective at
314 a short distance, the ephaptic transmission from the retinae may contribute significantly to firing rate
315 changes in downstream neurons of the photoreceptor cells in the optic lobe.

316 This study also revealed that odor responses of OSNs were clearly modulated when light
317 conditions changed transiently. This mechanism may help flies switch attention to newly presented sensory
318 cues or maintain attention toward those remaining after the change. Turning the light on, for example,
319 reduces the firing rates of the OSNs, which may enable the flies to pay more attention to visual information,
320 whereas turning the light off increases the firing rates of the OSNs, which may help them attend to olfactory
321 sensory cues.

322 Recent connectome analyses have revealed the entire synaptic network in the central nervous
323 system in *Drosophila* (Scheffer et al., 2020) and provides insight into how neural information is subject to
324 synaptic relays to determine the behavioral output. In this study, we show that ephaptic relays also
325 contribute to modulating the firing rate of distant neurons and modify the sensory responses that can change
326 momentarily in a context-dependent manner. To build an integrated model of the fly brain, we should also
327 consider ephaptic relay of neural information (Scheffer and Meinertzhagen, 2021). The compound
328 eye-antenna model would be a suitable model to determine the role of ephaptic transmission in neural
329 processing.

330

331 **References**

332 Anastassiou CA, Koch C (2015) Ephaptic coupling to endogenous electric field activity: why bother?
333 Curr Opin Neurobiol 31:95-103.

Bloomquist BT, Shortridge RD, Schneuwly S, Perdew M, Montell C, Steller H, Rubin GM, Pak WL (1988) Isolation of a putative phospholipase C gene of *Drosophila*, *norpA*, and its role in phototransduction. Cell 54:723-733.

Blot A, Barbour B (2014) Ultra-rapid axon-axon ephaptic inhibition of cerebellar Purkinje cells by the pinceau. Nature Neurosci 17:289-295.

Burg MG, Sarthy PV, Koliantz G, Pak WL (1993) Genetic and molecular identification of a *Drosophila* histidine decarboxylase gene required in photoreceptor transmitter synthesis. EMBO J 12:911-919.

Buzsáki G, Anastassiou CA, Koch C (2012) The origin of extracellular fields and currents-EEG, ECoG, LFP and spikes. Nat Rev Neurosci 13:407-20.

Choi KW, Benzer S (1994) Migration of glia along photoreceptor axons in the developing *Drosophila* eye. Neuron 12:423-431.

Chow DM, Theobald JC, Frye MA (2011) An olfactory circuit increases the fidelity of visual behavior. J Neurosci 31:15035-15047.

Dobritsa AA, van der Goes van Naters W, Warr CG, Steinbrecht RA, Carlson JR (2003) Integrating the molecular and cellular basis of odor coding in the *Drosophila* antenna. Neuron 37:827-841.

Faul F, Erdfelder E, Lang A-G, Buchner A (2007) G*Power 3: A flexible statistical power analysis program for the social, behavioral, and biomedical sciences. Behavior Research Methods 39:175-191.

Han KS, Guo C, Chen CH, Witter L, Osorno T, Regehr WG (2018) Ephaptic coupling promotes synchronous firing of cerebellar Purkinje cells. Neuron 100:564-578.

Kaissling KE, Thorson J (1980) Insect olfactory sensilla: structural, chemical and electrical aspects of the functional organization. In: Sattelle DB, Hall LM, Hildebrand JG, editors. Receptors for neurotransmitters, hormones and pheromones in insects. Amsterdam: Elsevier/North-Holland Biomedical Press. 261-282.

Malpel S, Klarsfeld A, Rouyer F (2002) Larval optic nerve and adult extra-retinal photoreceptors sequentially associate with clock neurons during *Drosophila* brain development. Development 129:1443-1453.

Melzig J, Buchner S, Wiebel F, Wolf R, Burg M, Pak WL, Buchner E (1996) Genetic depletion of histamine from the nervous system of *Drosophila* eliminates specific visual and mechanosensory behavior. J Comp Physiol A 179:763-773.

Ni JD, Baik LS, Holmes TC, Montell C (2017) A rhodopsin in the brain functions in circadian photoentrainment in *Drosophila*. Nature 545:340-344.

Olsson SB, Hansson BS. (2013) Electroantennogram and single sensillum recording in insect antennae. Methods Mol Biol 1068:157-177.

Pearn MT, Randall LL, Shortridge RD, Burg MG, Pak WL (1996) Molecular, biochemical, and electrophysiological characterization of *Drosophila norpA* mutants. J Biol Chem 271:4937-4945.

Scheffer LK, Xu CS, Januszewski M, Lu Z, Takemura SY, et al. (2020) A connectome and analysis of the adult *Drosophila* central brain. Elife 9:e57443.

Scheffer LK, Meinertzhagen IA (2021) A connectome is not enough - what is still needed to understand the brain of *Drosophila*? J Exp Biol 224(21).

Shanbhag SR, Müller B, Steinbrecht RA (1999) Atlas of olfactory organs of *Drosophila melanogaster* 1. Types, external organization, innervation and distribution of olfactory sensilla. Int J Insect Morph Embryology 28:377-397.

Stopfer M, Bhagavan S, Smith BH, Laurent G (1997) Impaired odour discrimination on desynchronization of odour-encoding neural assemblies. Nature 390:70-74.

Su CY, Menuz K, Reisert J, Carlson JR (2012) Non-synaptic inhibition between grouped neurons in an olfactory circuit. Nature 492:66-71.

Sweeney ST, Broadie K, Keane J, Niemann H, O'Kane CJ (1995) Targeted expression of tetanus toxin light chain in *Drosophila* specifically eliminates synaptic transmission and causes behavioral defects. Neuron 14:341-351.

Tachibana SI, Touhara K, Ejima A (2015) Modification of male courtship motivation by olfactory habituation via the $GABA_A$ receptor in *Drosophila melanogaster*. PLoS One 10: e0135186.

Takagawa K, Salvaterra P (1996) Analysis of choline acetyltransferase protein in temperature sensitive mutant flies using newly generated monoclonal antibody. Neurosci Res 24:237-243.

Tanaka NK, Ito K, Stopfer M (2009) Odor-evoked neural oscillations in *Drosophila* are mediated by widely branching interneurons. J Neurosci 29:8595-8603.

Tanaka NK, Suzuki E, Dye L, Ejima A, Stopfer M (2012) Dye fills reveal additional olfactory tracts in the protocerebrum of wild-type *Drosophila.* J Comp Neurol 520(18):4131-40.

van Atteveldt N, Murray MM, Thut G, Schroeder CE (2014) Multisensory integration: flexible use of general operations. Neuron 81:1240-1253.

van der Goes van Naters W, Carlson JR (2007) Receptors and neurons for fly odors in *Drosophila*. Curr Biol 17:606-612.

Weiss SA, Faber DS (2010) Field effects in the CNS play functional roles. Front Neural Circuits 4:15. doi: 10.3389/fncir.2010.00015.

Wernet MF, Labhart T, Baumann F, Mazzoni EO, Pichaud F, Desplan C (2003) Homothorax switches function of *Drosophila* photoreceptors from color to polarized light sensors. Cell 115: 267-279.

Wilson RI (2013) Early olfactory processing in *Drosophila*: Mechanisms and principles. Annu Rev Neurosci 36:217-241.

Yarali A, Mayerle M, Nawroth C, Gerber B (2008) No evidence for visual context-dependency of olfactory learning in *Drosophila*. Naturwissenschaften 95:767-774.

Yasuyama K, Meinertzhagen IA (1999) Extraretinal photoreceptors at the compound eye's posterior margin in *Drosophila melanogaster*. J Comp Neurol 412:193-202.

Zhang Y, Tsang TK, Bushong EA, Chu LA, Chiang AS, Ellisman MH, Reingruber J, Su CY (2019) Asymmetric ephaptic inhibition between compartmentalized olfactory receptor neurons. Nat Commun 10:1560.

410 **Figure legends**

411 **Figure 1. Transient changes in light condition modulated *cis*-vaccenyl acetate (cVA) response of**
412 **Or67d olfactory sensory neurons (OSNs) in wild-type flies**

413 ***A*,** Experimental setup. While recording spikes extracellularly from Or67d OSN, cVA and/or blue light
414 stimulations were applied to the fly's head. ***B*,** Extracellular recording of spikes from Or67d OSNs. The
415 upper panel shows the response to a sole cVA puff, whereas the lower panel shows the response to
416 simultaneous stimulation with cVA and blue light. The red lines indicate the timing of 3-s odor stimulations
417 and the blue line represents 1.5 s of lighting period. I, II, and III represent the first 50 ms after the light
418 condition was changed, 1.2 s while transient change in the light condition was sustained, and 300 ms just
419 after the light condition was returned to the original condition, respectively.

420
421 **Figure 2. Transient changes in the light condition modulated *cis*-vaccenyl acetate (cVA) responses**
422 ***A* and *B*,** Transient lighting (***A***) and darkening (***B***) during the latter half of odor stimulations changed the
423 firing rates of OSNs. The left panel shows the firing rates in each 300 ms bin. The blue and black lines
424 represent 1.5 s of the lighting and darkening periods, respectively. The right graphs indicate the firing rates
425 during I, II, and III, as shown in **Fig. 1*B***. n represents the number of animals recorded. ***C*,** Light responses of
426 the OSNs without odor stimulations. ***D*,** Transient lighting was applied during the first half of odor
427 stimulations. ***E*,** The cVA response under constant light or constant dark condition. The right panel shows
428 the firing rates during the first and second halves of the odor stimulations. For statistical analyses, Wilcoxon
429 matched-pairs signed rank test (***A***–***D***) and Mann-Whitney test (***E***) were performed. The error bars indicate
430 the standard error of the mean.

431

432 **Figure 3. Transient lighting during the latter half of *cis*-vaccenyl acetate (cVA) stimulations**
433 **modulated the responses of Or67d olfactory sensory neurons (OSNs)**

434 ***A*,** Wild type with its antennal nerve amputated. ***B*,** Wild type whose head except for the antenna being
435 recorded was painted black. ***C*,** *eyes absent* (*eya*^{2}) mutant. ***D*,** *histidine decarboxylase* (*hdc*^{JK910}) mutant. ***E*,**

436 *longGMR-GAL4*/*UAS-TNT*. Left panels: the firing rates in each 300 ms bin. The blue lines represent 1.5 s of
437 the lighting period, whereas red lines indicate the timing of 3-s odor stimulations. Light blue lines show the
438 firing rate when both odor and light stimulations were applied, whereas gray lines indicate those where odor
439 stimulations were solely applied. Right panels: the firing rates during I, II, and III, as shown in **Fig. 1*B***. For
440 statistical analyses, Wilcoxon matched-pairs signed rank tests were performed. Error bars indicate the
441 standard error of the mean. ***F*-*I***, Expression patterns of *longGMR-GAL4*. Photoreceptors in the ocelli
442 (arrowheads in ***F***) and eyelet (arrowheads in ***G*-*I***) neurons as well as in the retinae are labeled. Magenta in ***G***
443 and white in ***H*** represent anti-choline acetyltransferase (ChAT) antibodies, whereas white in ***F*** and ***I*** and
444 green in ***G*** indicate the presence of anti-GFP antibodies. The area surrounded by dotted square in ***G*** is
445 enlarged in ***H*** and ***I***. Dorsal side is on the top, lateral is represented on the left (***G*-*I***). OL, optic lobe. Single
446 frontal confocal sections (***H***, ***I***) and 3D-reconstructed images (***F***, ***G***) are shown. Scale bars = 10 μm (***H***) and
447 100 μm (***F***, ***G***). Genotype: *w*; +/*UAS-GFP*; *UAS-20XmCD8::GFP*/*longGMR-GAL4*.
448
449 **Figure 4. Ephaptic transmission mediates the light-evoked firing rate increase in the Or67d olfactory**
450 **sensory neurons (OSNs)**
451 ***A*-*C*,** Transient lighting was applied during the latter half of odor stimulations in *eya*^{2} mutants transplanted
452 with a wild-type eye (***A*,*C***) or *no receptor potential A* (*norpA*^{36}) mutant eye (***B***). In ***C***, ground electrode was
453 placed in the extracellular saline. The left panels show the firing rates in each 300-ms bin. Blue lines
454 represent 1.5 s of the lighting period, whereas red lines indicate the timing of 3-s odor stimulations. Right
455 panels indicate the firing rates during I, II, and III, as shown in **Fig. 1*B***. ***D*, Negative current (-10 nA)**
456 **injected into the optic lobe area caused firing rate increases of the OSNs during odor stimulations in**
457 ***eya*^{2} mutants.** For statistical analyses, Wilcoxon matched-pairs signed rank tests were performed. Error
458 bars indicate the standard error of the mean.
459
460 **Table legend**
461 **Table1. Detailed statistic values**

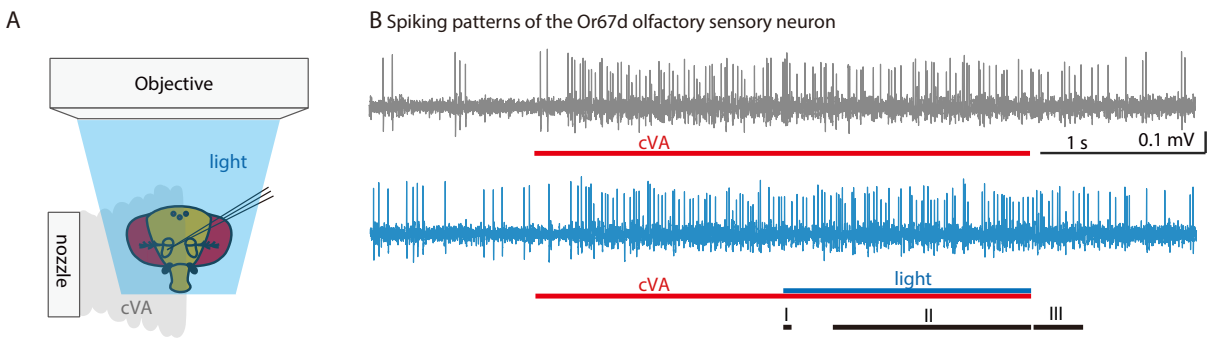

Figure 1

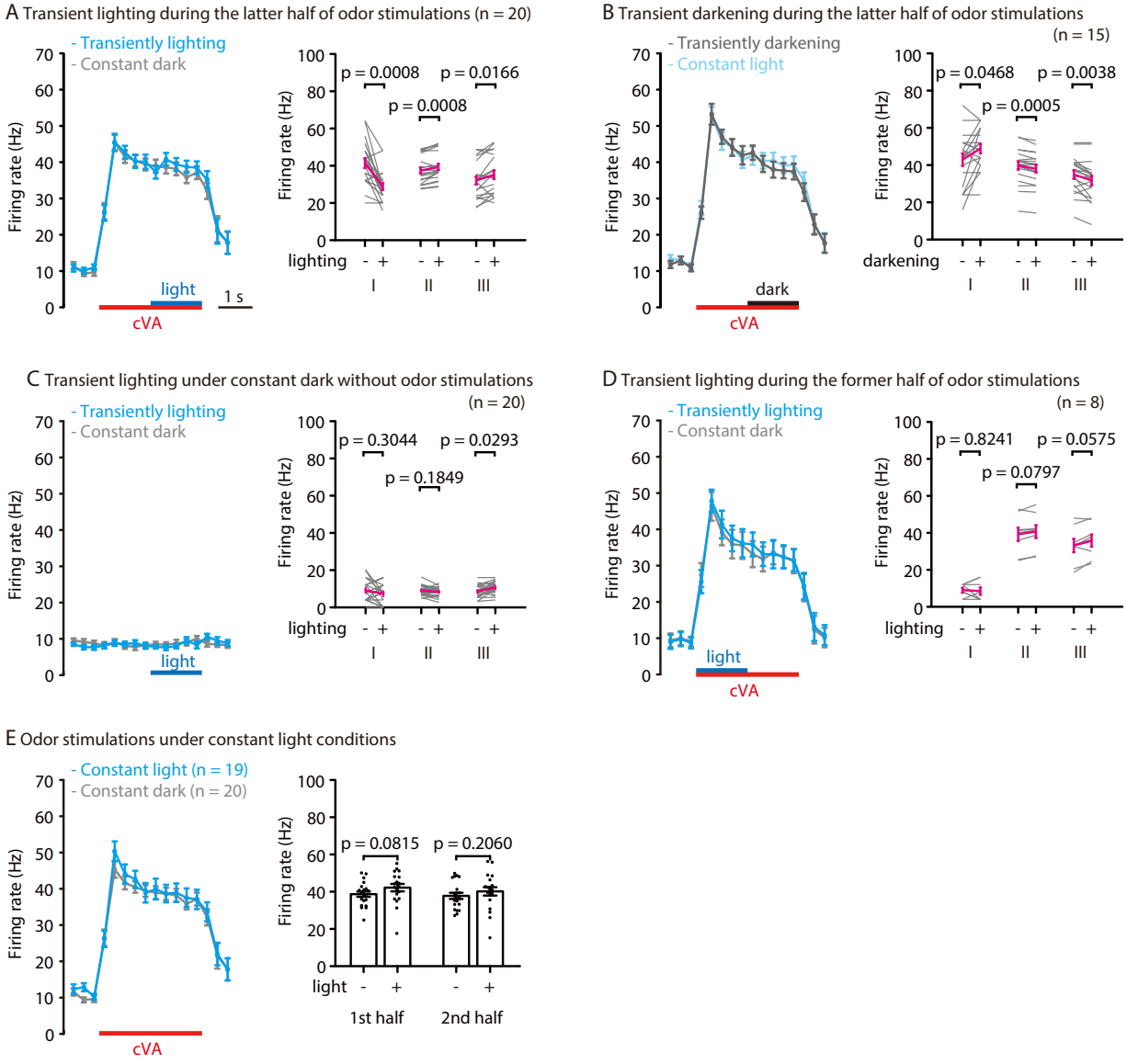

Figure 2

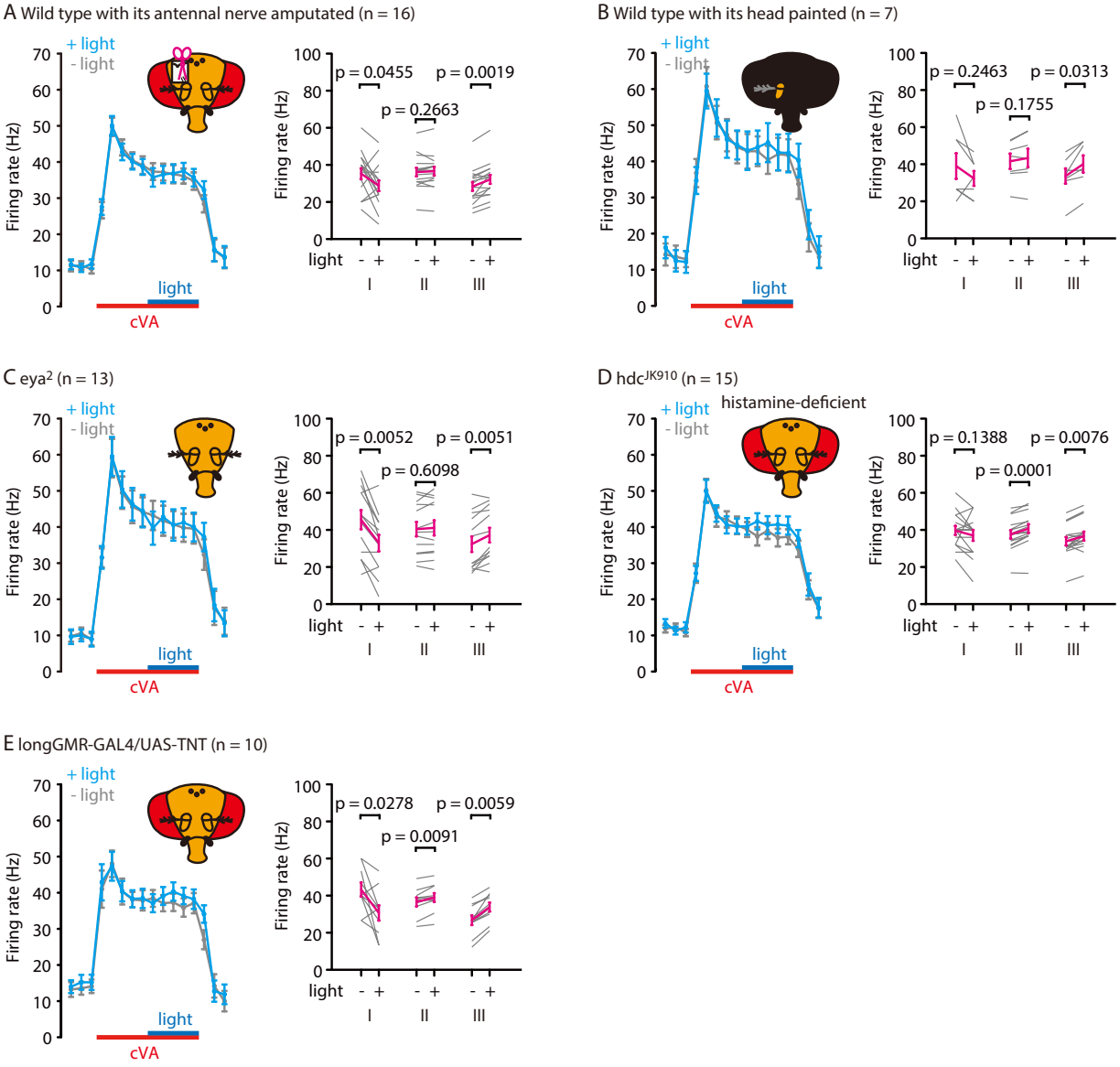

Figure 3

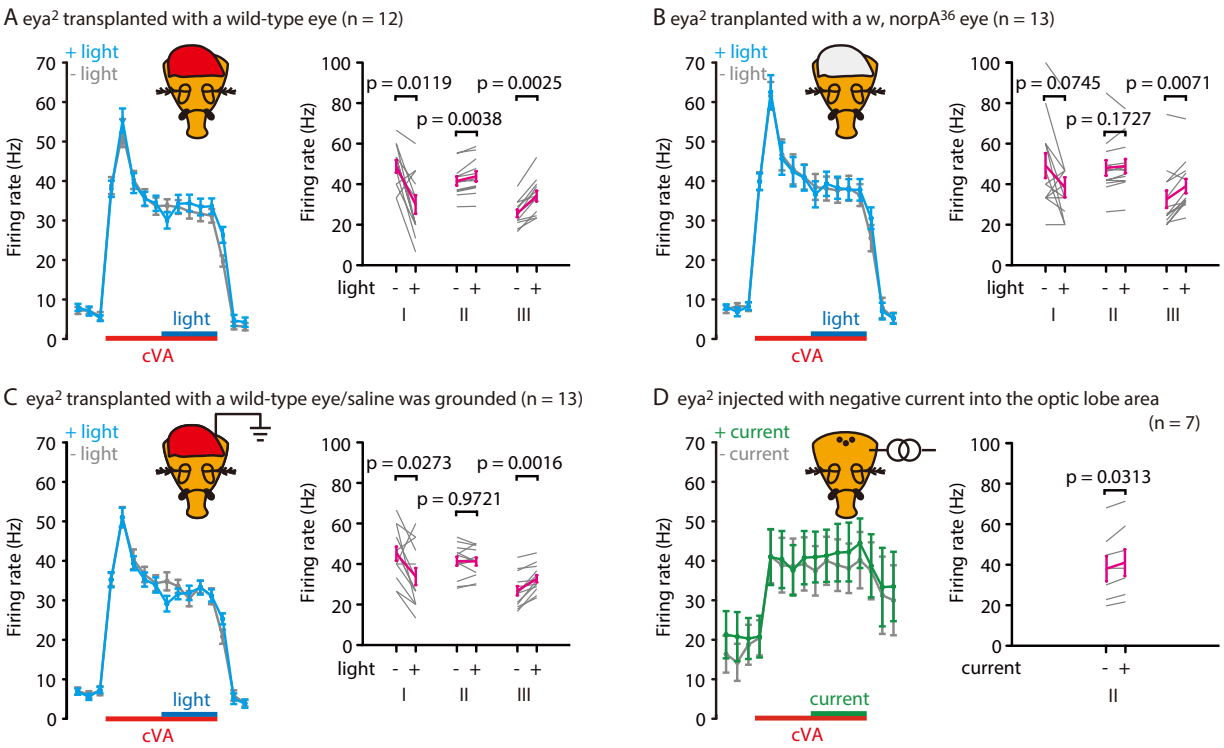

Figure 4

		I		II		III	
Wilcoxon matched-pairs signed rank test	Fig. 2A (n = 20)	W = 166 p = 0.0008	Z = 3.3623 r = 0.7518	W = -180 p = 0.0008	Z = -3.3608 r = 0.7515	W = -120 p = 0.0166	Z = 2.4349 r = 0.5445
	Fig. 2B (n = 15)	W = -64 p = 0.0468	Z = -2.0193 r = 0.4633	W = 161 p = 0.0005	Z = 3.5062 r = 0.8044	W = 123 p = 0.0038	Z = 2.8905 r = 0.6631
	Fig. 2C (n = 20)	W = 43 p = 0.3044	Z = 1.0514 r = 0.2351	W = 72 p = 0.1849	Z = 0.59753 r = 0.1336	W = -101 p = 0.0293	Z = -2.254 r = 0.5040
	Fig. 2D (n = 8)	W = 3 p = 0.8241	Z = 0.3333 r = 0.1179	W = -26 p = 0.0797	Z = 1.6824 r = 0.5948	W = -28 p = 0.0575	Z = -1.8927 r = 0.6692
	Fig. 3A (n = 16)	W = 71 p = 0.0455	Z = 2.029 r = 0.5073	W = -44 p = 0.2663	Z = -1.1376 r = 0.2844	W = -121 p = 0.0019	Z = -3.1326 r = 0.7832
	Fig. 3B (n = 7)	W = 12 p = 0.2463	Z = 1.4393 r = 0.5440	W = -17 p = 0.1755	Z = -1.0142 r = 0.3833	W = -21 p = 0.0313	Z = -2.2014 r = 0.8321
	Fig. 3C (n = 13)	W = 72 p = 0.0052	Z = 2.8317 r = 0.7854	W = -14 p = 0.6098	Z = -0.54934 r = 0.1524	W = -81 p = 0.0051	Z = -2.833 r = 0.7857
	Fig. 3D (n = 15)	W = 34 p = 0.1388	Z = 1.5251 r = 0.3938	W = -118 p = 0.0001	Z = -3.351 r = 0.8652	W = -86 p = 0.0076	Z = -2.668 r = 0.6889
	Fig. 3E (n = 10)	W = 44 p = 0.0278	Z = 2.2994 r = 0.7271	W = -45 p = 0.0091	Z = -2.6656 r = 0.8429	W = -55 p = 0.0059	Z = -2.8031 r = 0.8864
	Fig. 4A (n = 12)	W = 65 p = 0.0119	Z = 2.5515 r = 0.7366	W = -66 p = 0.0038	Z = -2.9821 r = 0.8609	W = -78 p = 0.0025	Z = -3.0606 r = 0.8835
	Fig. 4B (n = 13)	W = 41 p = 0.0745	Z = 1.8281 r = 0.5070	W = -40 p = 0.1727	Z = -1.3981 r = 0.3878	W = -78 p = 0.0071	Z = -2.6223 r = 0.7273
	Fig. 4C (n = 13)	W = 57 p = 0.0273	Z = 2.316 r = 0.6423	W = 2 p = 0.9721	Z = 0.0699 r = 0.0194	W = -91 p = 0.0016	Z = -3.1808 r = 0.8822
	Fig. 4D (n = 7)			W = 21 p = 0.0313	Z = -2.2014 r = 0.8321		
		1st half		2nd half			

Mann-Whitney test	Fig. 2E (n = 19-20)	U = 127.5 p = 0.0815	Z = -1.7562 r = 0.2812	U = 144.5 p = 0.2060	Z = -1.2786 r = 0.2047